

# Seismic Response Analysis of Joint-Connected Buried Pipelines Including Bent Sections

By

Hisao GOTO, Masata SUGITO, Hiroyuki KAMEDA\*, and Yutaka ISHIKAWA\*\*

(Received September 30, 1981)

## Abstract

Response analysis of joint-connected buried pipelines including bent sections has been carried out using analytical models, types of which are commonly used in the actual underground lifeline systems. The details of the structures and materials along the trunk routes of the Kyoto City Water Supply Districts have been intensively examined to establish these analytical models. Response analysis for four representative models of buried pipelines has been performed with some analytical parameters of pipe-structures, input ground motions, and soil springs, etc., focusing on the effects of the structural and input ground motion parameters on the response behavior of pipelines.

## 1. Introduction

It is an indispensable subject for a seismic risk assessment of underground lifeline systems to make clear the behavior of buried pipes during earthquakes. The effect of propagating seismic waves, one of the major causes of structural damage to buried pipes, has been studied by many authors (3,8,10,12,13,14,15,21, 22). Their results are generally summarized as follows. (1) The behavior of buried pipes is subject to the relative displacement of the ground, and the mass effect of pipes is negligible. (2) The axial strain is predominant in pipes compared with the bending strain. (3) The slippage between the pipes and surrounding soils makes the pipe strain smaller than in the case of no slippage. (4) At the bent and the crossing sections of the pipes, a relatively large stress occurs in comparison with the straight part of the pipes. (5) In the case of joint-connected pipes, the joint absorbs the ground strain, and the axial stress of the pipes rarely occurs in the expansion side when the joint is movable.

The analytical models of the pipes dealt with in past studies have been the straight parts of pipelines, and some works have dealt with curved pipes or junctions (8,12,14,15). In this work, the angle of bent pipes and the angle between

---

\* Respectively, Professor, Research Associate, and Associate Professor, Department of Transportation Engineering.

\*\* Research Institute of Shimizu Construction.

the direction of the pipe axis and that of the wave propagation have been analyzed for some specific cases (8,12). However, in the actual underground lifeline systems, the structural forms at the bent and junctional sections are usually not so simple as those of the analytical models.

Table 1 shows an example of typical structures which constitute the actual water supply system (in Kyoto City), and their seismic input characteristics which should be examined for their structural behavior during earthquakes. It is of importance for a seismic risk assessment of underground lifeline systems to estimate not only the structural behavior of buried pipes but that of some particular structures listed in Table 1.

This study deals with the response analysis of joint-connected buried pipelines

Table 1. Structural Characteristics of Water Supply Systems and Their Seismic Input Characteristics.

		schema	concerned section	input characteristics			
				wave propagation	acceleration of ground	permanent displacement of ground	liquefaction
buried pipeline	straight pipes			○		○	○
	bent pipes	horizontal		○		○	○
		vertical		○		○	○
		horizontal and vertical		○		○	○
	T junction		branch section	○		○	○
particular structural form	pipe bridge		crossing over river		○	○	
	pipes attached to bridge		crossing over river		○		
	L-junction		crossing over pipes	○		○	○
	disclosed pipes		provisionally distributed pipes		○	○	
	pipes jointed to structure		exit of supply plant	○		○	
	concrete pipe bridge		head gate of supply plant		○	○	
	pipes buried in embankment		embankment	○		○	

using analytical models, types of which are commonly used in the actual underground lifeline systems.

First, the details of the structures and materials along the trunk routes of the Kyoto City Water Supply Districts have been intensively examined to establish the analytical models of underground pipelines, whose structural forms are common in the actual systems. Four typical models of joint-connected buried pipelines including horizontal and vertical bent pipes have been established.

Next, response analysis of joint-connected pipelines has been carried out with some analytical parameters of pipe-structures, input ground motions, and soil springs, etc., focusing on the effect of structural and input ground motion parameters on the response behavior of pipelines.

## **2. Structural Characteristics of Buried Pipeline Systems and Typical Models for Response Analysis**

### **2.1 Structural characteristics of trunk routes of water supply system in Kyoto City**

The details of the structures and materials of the aqueducts and some parts of the Kyoto City Water Supply Districts have been examined to establish the analytical models, types of which are common in the actual systems.

Fig. 1 shows the aqueducts and the water supply districts in Kyoto City. In Fig. 1, the aqueducts and the trunk routes in zones [5] and [11] have been surveyed, focusing on the materials and the diameters of pipes, the angle of the bent pipes, the structural forms at the bent and crossing sections, and the types of joints, etc. Fig. 2 shows the percentage of pipe materials in the total length of construction and that of bent angles in horizontal and vertical bent pipes.

In the survey on the trunk routes of the Kyoto City Water Supply System, the following articles of its structural and material characteristics have been summarized.

- (1) The trunk routes consist mostly of ductile iron pipes (DAK), and partly of steel pipes (SP), concrete pipes (RC), and cast iron pipes (CIP).
- (2) The bent pipes are used mainly in horizontal and vertical directions, and the bent angles, in the case of ductile iron pipes, are of 5 types, namely  $90^\circ$ ,  $45^\circ$ ,  $22\frac{1}{2}^\circ$ ,  $11\frac{1}{4}^\circ$ , and  $5\frac{5}{8}^\circ$ . Bent pipes for  $45^\circ$  and  $22\frac{1}{2}^\circ$  are used most frequently, and those for  $90^\circ$ , which have been often applied in the analytical models of pipelines including bent sections (7,11,13,14), are very few.
- (3) A couple of bent pipes are commonly used for bent sections, such as two  $45^\circ$  bent pipes for a  $90^\circ$  bent section (Fig. 3).



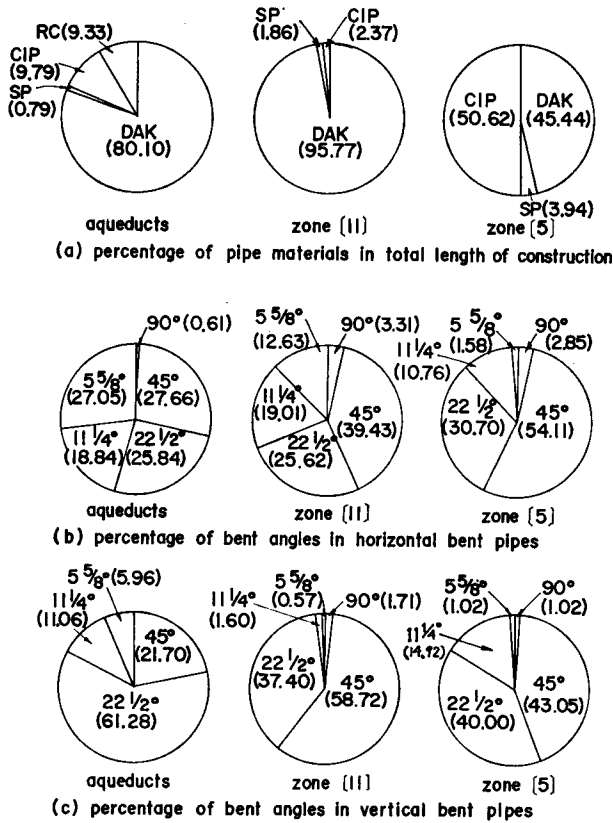


Fig. 2. Percentage of Pipe Materials and Angles of Bent Pipes in Kyoto City Water Supply System (aqueducts, zone [5], zone [11]).

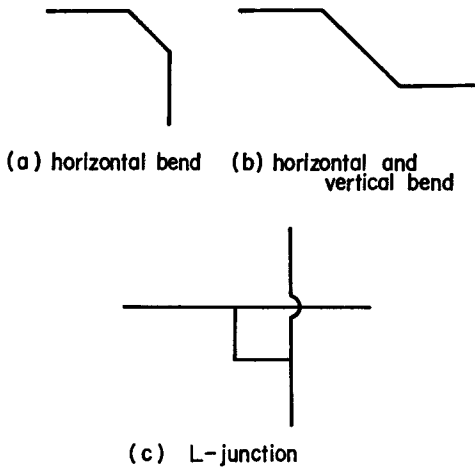


Fig. 3. Typical Structural Forms at Bent and Crossing Sections.

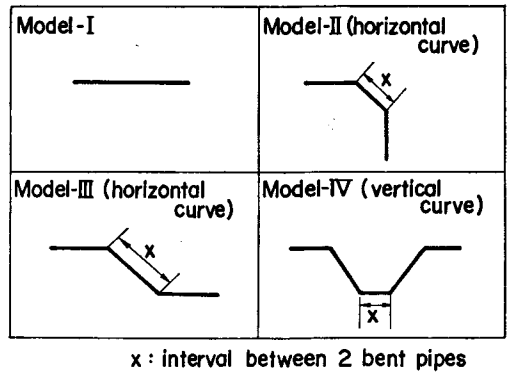


Fig. 4. Typical Models of Buried Pipelines.

lifeline system (Kyoto City Water Supply System), four typical models of buried pipelines have been established. In Fig. 4, Model-I represents the straight part of the pipes, and Models-II and III represent the horizontal curved sections where a couple of bent pipes are commonly used. Model-IV is a vertical curved section, which is used where the pipeline passes under rivers, buried structures, etc.

*Computational parameters in response analysis*

a) Input ground motion

The longitudinal waves represented by horizontally propagating sinusoidal waves are dealt with in the response analysis. The wave length  $L$  is fixed as  $L=120$  m, with reference to the Guide and Commentary for Earthquake Resistant Construction Code of Water Supply Facilities (4). The amplitude of the ground displacement  $u_m$  is varied as  $u_m=1,2,4,8$  cm. From these values of  $L$  and  $u_m$ , the maximum free field normal strain  $\epsilon_{max}$  takes the values  $\epsilon_{max}=0.52, 1.05, 2.09,$  and  $4.19 \times 10^{-4}$ . Several cases are considered for the angle of incidence of waves to the pipe. The vertical distribution of the ground displacement is considered in the response analysis of Model-IV. A free field displacement is supposed to decrease linearly in the vertical direction, and the amplitude at depth 5 m of the ground motion is fixed at 95 % of that at depth 1 m, after Toki (18) and Kamiyama (5).

b) Soil springs

In the Earthquake Resistant Construction Code(4) the soil springs are given as follows:

$$\begin{aligned} K_{g1} &= k_{g1}G_s \\ K_{g2} &= k_{g2}G_s \end{aligned} \quad (1)$$

where  $K_{g1}, K_{g2}$  are the soil spring constants ( $\text{kg}/\text{cm}^2$ ) for the unit length in the axial and the transverse directions of pipes, respectively.  $k_{g1}, k_{g2}$  are the constants with a value around 3, and  $G_s$  is the shear modulus of the soil ( $\text{kg}/\text{cm}^2$ ) which is estimated from

$$G_s = (\gamma_t/g) \cdot V_s^2 \quad (2)$$

where  $\gamma_t$  is the weight of soil per unit volume ( $\text{kg}/\text{cm}^3$ ),  $g$  is the acceleration of gravity ( $=980 \text{ cm}/\text{sec}^2$ ), and  $V_s$  is the shear velocity ( $\text{cm}/\text{sec}$ ) of the soil around the pipe. From Eqs. (1) and (2) the soil spring constants  $K_{g1}, K_{g2}$  are given as:

$$K_{g1} = K_{g2} = 3(\gamma_t/g)V_s^2 \quad (3)$$

Using the boring data (7) for Kyoto City provided for each  $500 \text{ m} \times 500 \text{ m}$  mech, the distribution of the shear modulus  $G_s$  of the surface layer has been obtained as shown in Fig. 5. The shear velocity  $V_s$  in Eq. (2) has been estimated

from the formulas in Table 2. The weight per unit volume  $\gamma_t$  has been given as in Table 3. From these results, three values of soil spring constants, with respect to the softness of soil, have been determined as:

$$\begin{aligned}
 K_{g1}, K_{g2} &= 1200 \text{ (kg/cm}^2\text{)} \text{ for relatively hard soil} \\
 &= 750 \text{ (kg/cm}^2\text{)} \text{ for intermediate soil} \\
 &= 300 \text{ (kg/cm}^2\text{)} \text{ for soft soil}
 \end{aligned}$$

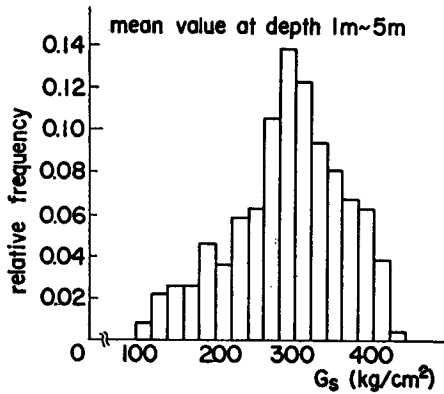


Fig. 5. Histogram for Estimated Shear Modulus  $G_s$  of Surface Layer in Kyoto City.

Table 2. Estimation Equations for Shear Velocity  $V_s^{(2)}$ .

diluvium	clay	$129N^{0.183}$
	sand	$123N^{0.125}$
alluvium	clay	$122N^{0.0777}$
	sand	$61.8N^{0.211}$

(N; blow-count)

Table 3. Estimation Values for a Weight per Unit Volume.

clay, silt	sand	gravel, rock
1.6	1.7	1.8

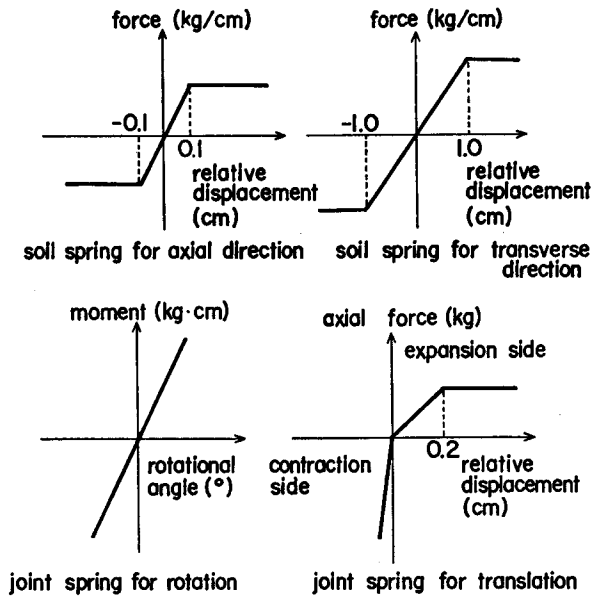


Fig. 6. Typical Soil and Joint Spring Characteristics Used in Response Analysis.

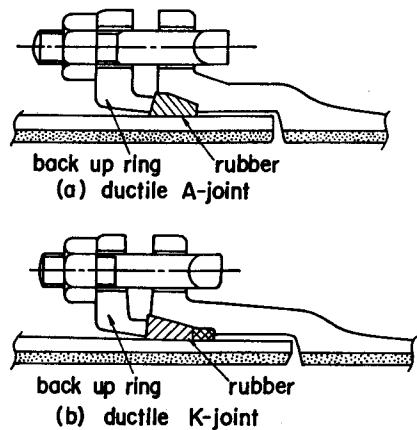


Fig. 7. Typical Pipe Joints.

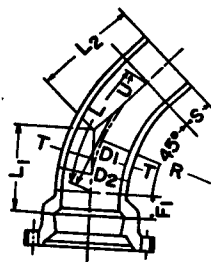
Table 4. Dimensions of Straight Pipes.

nominal diameter		1650	800	400
outside diameter	(cm)	170.1	83.6	42.56
thickness of pipe	(cm)	2.25	1.2	0.75
inside diameter	(cm)	165.6	81.2	41.06
cross sectional area	(cm <sup>2</sup> )	1186.5	310.6	98.5
geometrical moment of inertia	(cm <sup>4</sup> )	4.18×10 <sup>6</sup>	2.64×10 <sup>5</sup>	2.15×10 <sup>4</sup>
unit length	(cm)	400	600	600
Young's modulus	(kg/cm <sup>2</sup> )	1.6×10 <sup>6</sup>	1.6×10 <sup>6</sup>	1.6×10 <sup>6</sup>
joint spring	expansion side (kg/cm)	5.0×10 <sup>4</sup>	3.0×10 <sup>4</sup>	1.75×10 <sup>4</sup>
	contraction side (kg/cm)	2.0×10 <sup>6</sup>	2.0×10 <sup>6</sup>	2.0×10 <sup>6</sup>
	rotational spring (kg·cm/°)	4.0×10 <sup>5</sup>	4.0×10 <sup>5</sup>	4.0×10 <sup>5</sup>

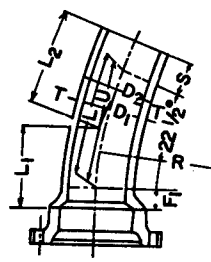
Table 5. Dimensions of Bent Pipes.

(unit ; mm)

	nominal diameter	thicknes	outside diameter	inside diameter	dimension of sections						
	D	T	D <sub>2</sub>	D <sub>1</sub>	L	R	S	U	F <sub>1</sub>	L <sub>1</sub>	L <sub>1</sub>
45°	1650	28.0	1701	1645	1178.1	1500	300	1148.1	80.3	701.6	921.3
	800	18.0	836.0	800.0	1335.1	1700	200	1301.1	60.6	764.8	904.2
	400	14.0	425.6	397.6	706.8	900	200	688.8	50.2	423.0	572.8
22½°	1650	28.0	1701	1645	1178.1	3000	300	1170.5	80.3	677.0	896.7
	800	18.0	836.0	800.0	1335.1	3400	200	1326.6	60.6	736.9	876.3
	400	14.0	425.6	397.6	706.8	1800	200	702.3	50.2	408.2	558.0



45° bent pipe




22 ½° bent pipe



Table 6(a). Computational Cases of Analytical Model (Model-I).

model-I — case number	nominal diameter (mm)			soil spring (kg/cm <sup>2</sup> )			angle of incidence (°)
	1650	800	400	1200	750	300	
101122111		○			○		0
102122121		○			○		90
103122131		○			○		45
104132111			○		○		0
105112111	○				○		0
106131111			○	○			0
107133111			○			○	0
191122111		○			○		0

Table 6(b). Computational Cases of Analytical Model (Model-II).

model-II  case number	bent angle (°)	nominal diameter (mm)			soil spring (kg/cm <sup>2</sup> )			interval between 2 bent pipes (m)				
		1650	800	400	1200	750	300	0	12	30	60	
201322113	45		○			○			○			
202322123	45		○			○			○			
203322133	45	○				○			○			
204312113	45			○		○			○			
205332113	45			○		○			○			
206232113	22½			○		○			○			
207332112	45			○		○						○
208332114	45			○		○		○				
209331112	45			○	○							○
210331113	45			○	○				○			
211331114	45			○	○			○				
212333112	45			○			○					○
213333113	45			○			○		○			
214333114	45			○			○	○				
215331115	45			○	○							○
216332115	45			○		○						○
217333115	45			○			○					○
292322113	45		○			○			○			

The relative displacement, at which slippage between the pipes and surrounding soil occurs, is fixed as  $d_s=0.1$  cm, after Toki (19) and Takada (16). The soil spring characteristics used in the response analysis are shown in Fig. 6.

c) Structural parameters of pipes

Ductile iron pipes, which are commonly used in the actual water supply systems, are applied for numerical analysis. The details of the straight and bent pipes used for the response analysis are listed in Tables 4 and 5. The spring characteristics of joints, which have been obtained from the results of the experimental tests (1,6) for the A and K-type joints of ductile iron pipes, are shown in Fig. 6. In this figure, the spring characteristics of the joints differ in the expansion and compression sides. The relative displacement at which slippage occurs at

Table 6(c). Computational Cases of Analytical Model (Model-III).



model-III  case number	bent angle (°)	nominal diameter (mm)			soil spring (kg/cm <sup>2</sup> )			interval between 2 bent pipes (m)			
		1650	800	400	1200	750	300	0	12	30	60
301322113	45		○			○			○		
302322123	45		○			○			○		
303322133	45		○			○			○		
304312113	45	○				○			○		
305332113	45			○		○			○		
306232113	22½			○		○			○		
307332112	45			○		○					○
308332114	45			○		○		○			
309331112	45			○	○						○
310331113	45			○	○				○		
311331114	45			○	○			○			
312333112	45			○			○				○
313333113	45			○			○		○		
314333114	45			○			○	○			
315331115	45			○	○					○	
316332115	45			○		○				○	
317333115	45			○			○			○	

Table 6(d). Computational Cases of Analytical Model (Model-IV).

model-IV  case number	bent angle (°)	nominal diameter (mm)			soil spring (kg/cm <sup>2</sup> )			angle of incidence (°)	interval between 2 bent pipes (m)			
		1650	800	400	1200	750	300		12	36	60	120
401322113	45		○			○		0		○		
402322123	45		○			○		90		○		
403322133	45		○			○		45		○		
404312113	45	○				○		0		○		
405332113	45			○		○		0		○		
406232113	22½			○		○		0		○		
407332112	45			○		○		0				○
408332114	45			○		○		0	○			
409331112	45			○	○			0				○
410331113	45			○	○			0		○		
411331114	45			○	○			0	○			
412333112	45			○			○	0				○
413333113	45			○			○	0		○		
414333114	45			○			○	0	○			
415331115	45			○	○			0				○
416332115	45			○		○		0				○
417333115	45			○			○	0				○

joints is fixed as 0.2 cm(6). Fig. 7 shows the A and K-type joints which are commonly used in the actual systems, and also the typical models of the joints used in the response analysis.

The computational cases of each model of pipelines are listed in Table 6(a)-(d).

### 3. Response analysis of buried pipelines

#### 3.1 Response analysis of joint-connected buried pipelines using transfer matrix method (11)

Response analysis of joint-connected buried pipelines are carried out in this chapter. The computational programs used in this study are based on ERAUL (1), developed by Takada (16).

*Analytical models*

Analytical models are constructed under the following condition:

- 1) Quasi-static analysis can be applied, i.e. the effect of the inertia forces and damping are assumed to be negligible.
- 2) Buried pipelines are treated as a series of segmented elastic beams, connected longitudinally with joints which have a non-linear spring behavior for both axial and bending motions. Each beam is supported by soil springs with sliding characteristics.
- 3) Seismic forces, generated by soil deformation relative to pipe motions, act on the pipe body through the soil spring.
- 4) The pipe motions are analyzed within a two dimensional horizontal plane, and a perfect elastic behavior is assumed for the pipe material.

Fig. 8 shows the analytical model of buried pipes.

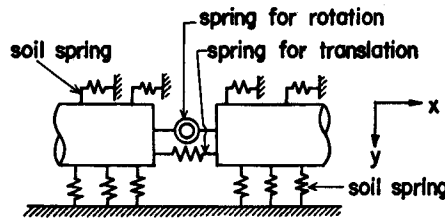


Fig. 8. Analytical Model for Buried Pipes.

*Equations of motion and their solutions*

Differential equations can be established with respect to the internal force within the pipe, and the force proportional to the displacement of the pipe relative to those of the free field:

- 1) longitudinal motion

$$-EA \frac{d^2u}{dx^2} + k_{s_x} \cdot u = k_{s_x} \cdot u_{s_x} \tag{4}$$

- 2) transverse motion

$$EI \frac{d^4v}{dx^4} + k_{s_y} \cdot v = k_{s_y} \cdot u_{s_y} \tag{5}$$

where  $u, v$  = the longitudinal and transverse displacements of the pipe,  $u_{s_x}, u_{s_y}$  = the longitudinal and transverse displacements of the free fields, respectively,  $E$  = Young's modulus of the pipe material,  $A, I$  = the cross sectional area and geometrical moment of inertia of the pipe, respectively,  $k_{s_x}, k_{s_y}$  = the equivalent spring constants for the longitudinal and transverse motions, respectively, to reflect the soil-structure interaction.

Eqs. (4) and (5) are rewritten as follows, using the free field displacement represented by a sinusoidal wave with an arbitrary incident angle  $\theta$  to the longitudinal axis ( $x$ -axis) of the pipeline:

1) longitudinal motion

$$-EA \frac{d^2 u}{dx^2} + k_{s_x} u = k_{s_x} u_{s_{x_0}} \sin \left[ \omega \cdot \left\{ t - \frac{(x+\xi) \cos \theta}{c} \right\} \right] \quad (6)$$

2) transverse motion

$$EI \frac{d^4 v}{dx^4} + k_{s_y} v = k_{s_y} u_{s_{y_0}} \sin \left[ \omega \cdot \left\{ t - \frac{(x+\xi) \cos \theta}{c} \right\} \right] \quad (\text{See Fig. 9}) \quad (7)$$

where  $u_{s_{x_0}}$  and  $u_{s_{y_0}}$  = the longitudinal and transverse displacement amplitudes of the free field,  $\omega$  = angular frequency,  $c$  = apparent wave speed,  $\xi$  = distance which results from a phase delay at the origin of  $x$ -axis. In Eqs. (6) and (7), the displacement amplitudes  $u_{s_{x_0}}$  and  $u_{s_{y_0}}$  are represented by the free field displacement amplitude  $u_m$ :

$$\begin{aligned} u_{s_{x_0}} &= u_m \cos \theta \\ u_{s_{y_0}} &= -u_m \sin \theta \end{aligned} \quad (8)$$

The general solutions  $u(x)$  and  $v(x)$  in Eqs. (6) and (7) are obtained as follows:

$$v(x) = e^{\beta_1 x} (C_1 \cos \beta_1 x + C_2 \sin \beta_1 x) + e^{\beta_1 x} (C_3 \cos \beta_1 x + C_4 \sin \beta_1 x) + v_0(x) \quad (9)$$

$$u(x) = C_5 \cosh \beta_2 x + C_6 \sinh \beta_2 x + u_0(x) \quad (10)$$

where

$$\beta_1 = (k_{s_y}/4EI)^{1/4} \quad (11)$$

$$\beta_2 = (k_{s_x}/EA)^{1/2} \quad (12)$$

$$v_0(x) = \frac{u_{s_{y_0}}}{1 + \frac{EI}{k_{s_y}} (\omega \cos \theta / c)^4} \sin \left[ \omega \cdot \left\{ t - \frac{(x+\xi) \cos \theta}{c} \right\} \right] \quad (13)$$

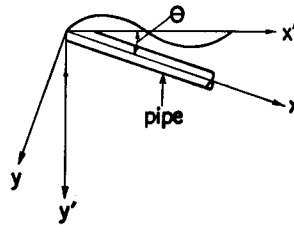


Fig. 9. Buried Pipe and Horizontally Propagating Seismic Wave.

$$u_0(x) = \frac{u_{s0}}{1 + \frac{EA}{k_{sx}} (\omega \cos \theta / c)^2} \sin \left[ \omega \cdot \left\{ t - \frac{(x + \xi) \cos \theta}{c} \right\} \right] \quad (14)$$

and  $C_1 \sim C_6$  are the constants of integration to be determined by the boundary conditions.

Then, the physical quantities such as the deflections  $u$  and  $v$ , the deflection angle  $\phi$ , the axial force  $N$ , the moment  $M$ , and the shear force  $Q$  at an arbitrary point  $x$  are obtained, using the boundary conditions  $u^L, v^L, \phi^L, N^L, M^L$ , and  $Q^L$ .

$$u(x) = u^L \beta_5(x) - N^L \frac{B_6(x)}{EA \beta_2} + D_5(x) \quad (15)$$

$$v(x) = v^L B_1(x) - \frac{\phi^L}{2\beta_1} B_3(x) + \frac{M^L}{2\beta_1^2 EI} B_2(x) - \frac{Q^L}{4\beta_1^3 EI} B_4(x) + D_1(x) \quad (16)$$

$$\phi(x) = -v^L \beta_1 B_4(x) + \phi^L B_1(x) - \frac{M^L}{2\beta_1 EI} B_3(x) - \frac{Q^L}{2\beta_1^2 EI} B_2(x) + D_2(x) \quad (17)$$

$$N(x) = -u^L EA \beta_2 B_6(x) + N^L B_5(x) + D_6(x) \quad (18)$$

$$M(x) = -2v^L EI \beta_1^2 B_2(x) - \phi^L \beta_1 EIB_4(x) + M^L B_1(x) + \frac{Q^L}{2\beta_1} B_3(x) + D_3(x) \quad (19)$$

$$Q(x) = -2v^L EI \beta_1^3 B_3(x) + 2\phi^L \beta_1^2 EIB_2(x) + M^L \beta_1 B_4(x) + Q^L B_1(x) + D_4(x) \quad (20)$$

In Eqs. (15)~(20), the functions  $B_1(x) \sim B_6(x)$  and  $D_1(x) \sim D_6(x)$ , which are called load terms, are represented in Appendix A. The positive directions of the forces  $N^L, Q^L, M^L$ , etc. in  $i$ -th beam are shown in Fig. 10.

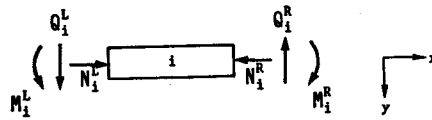


Fig. 10. Positive Direction of Forces

#### Transfer matrix method

Substituting  $x=l$ , which is the length of the unit pipe, into Eqs. (15)~(20), the relationship between the physical quantity  $\mathbf{V}^R$  on the right side of the  $i$ -th beam and  $\mathbf{V}^L$  on the left side is given as:

$$\mathbf{V}^R = \mathbf{FV}^L \quad (21)$$

where  $\mathbf{V}^R$  and  $\mathbf{V}^L$ , called state vectors, are the column vectors of physical quantities such as the deflections,  $u$  and  $v$ , the deflection angle  $\phi$ , the axial force  $N$ , the moment  $M$ , and the shear force  $Q$  at the ends of the right and left side of  $i$ -th beam, and  $\mathbf{F}$  is the field matrix which has the function of transferring the state vector

from one end to the other of the beam.

Next, the equilibrium equations at the joints are given by

$$\begin{pmatrix} u \\ v \\ \phi \end{pmatrix}_{k+1}^L = \begin{pmatrix} u \\ v \\ \phi \end{pmatrix}_k^R + \begin{pmatrix} -N/k_T \\ -M/k_R \\ 0 \end{pmatrix}_k^R, \quad \begin{pmatrix} N \\ M \\ Q \end{pmatrix}_{k+1}^L = \begin{pmatrix} N \\ M \\ Q \end{pmatrix}_k^R \quad (22)$$

where  $k_T$  and  $k_R$  are translational (longitudinal) and rotational springs representing the mechanical features of the joints. Eqs. (22) is rewritten as follows:

$$\mathbf{V}_{k+1}^L = \mathbf{P}_k \mathbf{V}_k^R \quad (23)$$

where  $\mathbf{P}_k$  is the point matrix which relates  $\mathbf{V}_{k+1}^L$  with  $\mathbf{V}_k^R$ . (See Appendix A.)

The equilibrium state of the deformations and forces at the bent sections are shown in Fig. 11. The following relations for the deformations and forces at the bent sections of the pipes are obtained using the bent angle  $\alpha$  of the pipelines.

$$\begin{cases} N_{k+1}^L = N_k^R \cos \alpha + Q_k^R \sin \alpha \\ Q_{k+1}^L = -N_k^R \sin \alpha + Q_k^R \cos \alpha \\ M_{k+1}^L = M_k^R \end{cases} \quad (24)$$

$$\begin{cases} u_{k+1}^L = -N_k^R \cos \alpha / k_T - Q_k^R \sin \alpha / k_T + u_k^R \cos \alpha + v_k^R \sin \alpha \\ v_{k+1}^L = v_k^R \cos \alpha - u_k^R \sin \alpha \\ \phi_{k+1}^L = \phi_k^R - M_k^R / k_R \end{cases} \quad (25)$$

The point matrix  $\mathbf{P}$  at the bent sections is given from Eqs. (24) and (25). (See Appendix A.) The boundary condition at the left hand side of the pipeline is represented by the boundary matrix  $R$  and the initial matrix  $\mathbf{A}_1^L$  as

$$\mathbf{V}_1^L = \mathbf{R} \mathbf{A}_1^L \quad (26)$$

In Eq. (26), the members of the initial vector  $\mathbf{A}_1^L$  represent the degree of freedom. In the response analysis of this study, the hinged condition is used at the ends of both sides to neglect the influence of the boundary conditions on the computational

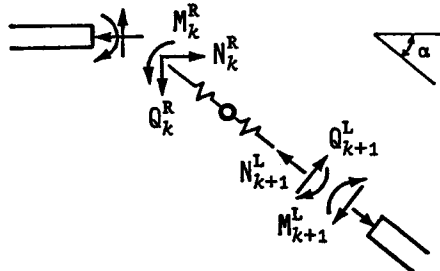


Fig. 11. Equilibrium State of Forces at Bent Section.

results of the response analysis. Then,  $\mathbf{R}$ ,  $\mathbf{A}_1^L$ , and the boundary matrix  $\mathbf{R}'$ , at the right hand side, are represented as follows.

$$\mathbf{R}^T = \begin{pmatrix} 0 & 0 & 0 & 1 & 0 & 0 & 0 \\ 0 & 0 & 1 & 0 & 0 & 0 & 0 \\ 0 & 0 & 0 & 0 & 0 & 1 & 0 \\ u_{sx}(0, t) & u_{sy}(0, t) & 0 & 0 & 0 & 0 & 1 \end{pmatrix}, \quad \mathbf{A}_1^L = \begin{pmatrix} N \\ \phi \\ Q \\ 1 \end{pmatrix}_1,$$

$$\mathbf{R}' = \begin{pmatrix} 1 & 0 & 0 & 0 & 0 & 0 & -u_{sx}(nl, t) \\ 0 & 1 & 0 & 0 & 0 & 0 & -u_{sy}(nl, t) \\ 0 & 0 & 0 & 0 & 1 & 0 & 0 \end{pmatrix} \quad (27)$$

The boundary condition at the right hand side of the line is represented by using the boundary matrix  $\mathbf{R}'$  as:

$$\mathbf{R}'\mathbf{V}_N = 0 \quad (28)$$

Substituting the boundary conditions of Eqs. (26) and (28) into the relations of Eqs. (21) and (23), the next linear equation can be obtained.

$$\mathbf{R}' \cdot \mathbf{F}_N \cdot \mathbf{P}_{N-1} \cdot \mathbf{F}_{N-1} \cdots \mathbf{P}_1 \cdot \mathbf{R} \cdot \mathbf{A}_1^L = 0 \quad (29)$$

In Eq. (29), the solution for  $\mathbf{A}_1^L$  is given, and then all unknown variables can be obtained with the aid of the field and point matrices.

### 3.2 Computational results and discussions

Using the analytical method just mentioned above, numerical computations have been carried out for the typical cases listed in Table 6(a)~(d). For numerical computations, the ERAUL(1), developed by Takada (16) for the response analysis of buried pipelines, has been used.

The details in the analytical procedures are as follows.

- (1) The pipe is separated into 1 m segments for the straight part, and the bent pipe is separated into 5 segments for the 45° pipe and 3 segments for the 22½° pipe.
- (2) The load increment method, which assumes the behavior of the system to be linear within a certain range of the input displacement, has been used as a numerical computational technique for the non-linear behavior of the soil and joint springs. The number of load increment steps are 10, 20, 40, and 80 for the input displacement amplitudes 1,2,4, and 8 cm, respectively.
- (3) At the both ends of the analytical models, the pipes are assumed to move just the same as the ground motions, not being restricted for the rotational force; i.e., the boundary condition for both ends of the pipelines is a hinge.



Discussions are focused on the effects of the following items on the behavior of pipelines during earthquakes.

- [1] Joint-structures of pipelines
- [2] Bent pipes, angle of bent pipes, and interval of two bent pipes
- [3] Diameter of pipes
- [4] Soil springs
- [5] Wave length and amplitude of input displacement
- [6] Angle of incidence and phase of input displacement

[1] *Joint-structures of pipelines*

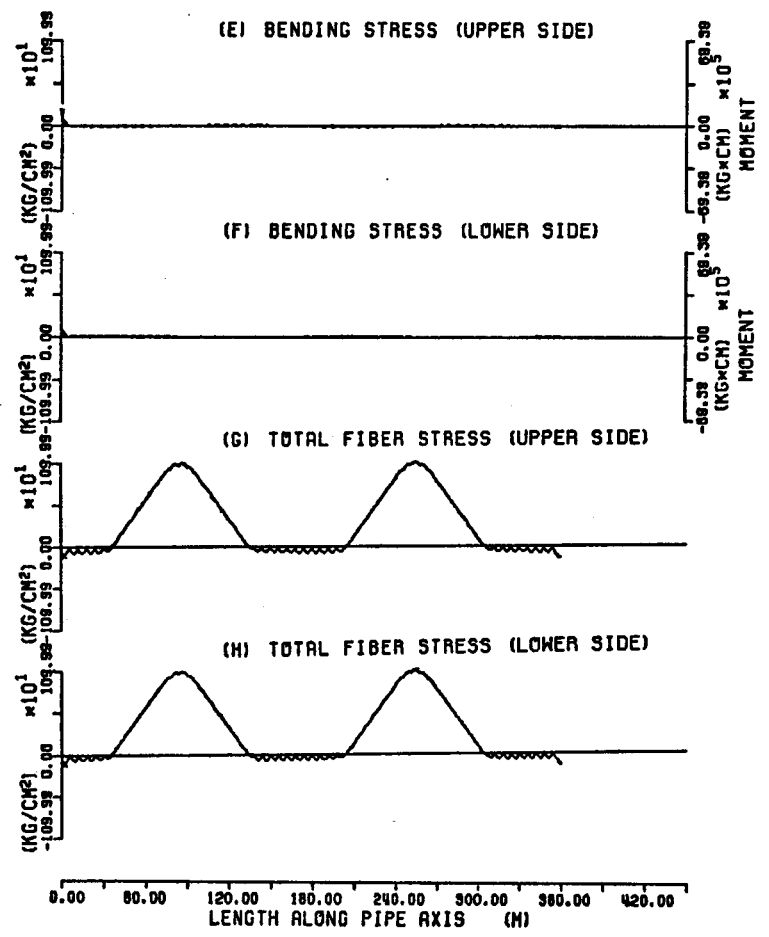
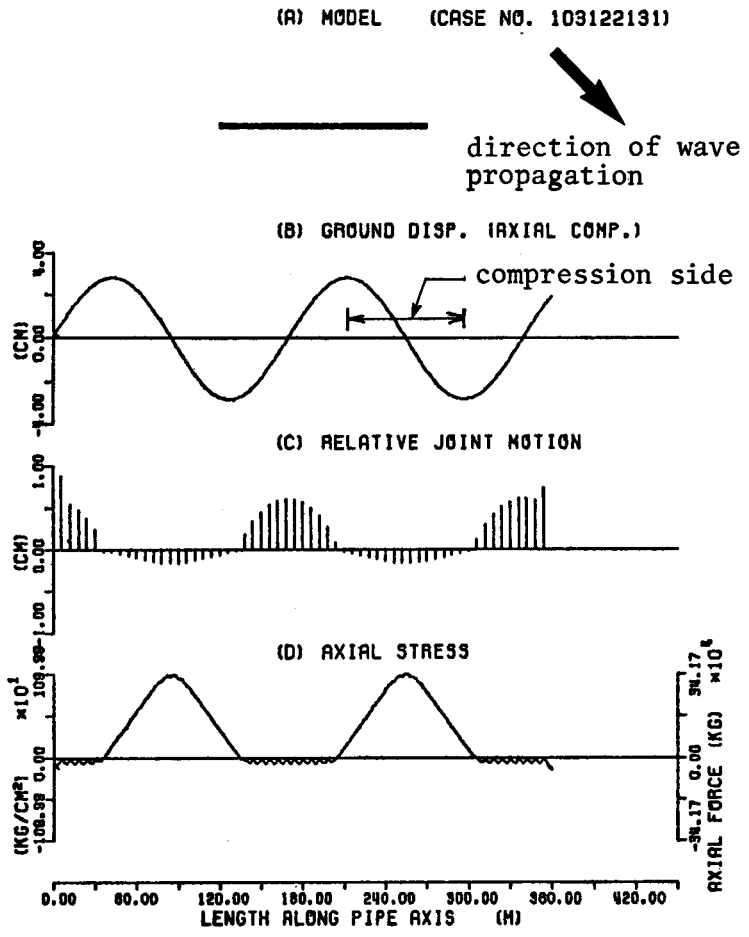
Fig. 12 shows an example for the distributions of the response values for Model-I. The abscissa represents a length in the axial component. In Fig. 12, the axial stress has larger values on the compression side of the ground strain, where the joints can not be pushed in easily, as shown in Fig. 6. In contrast with this, the relative joint motions are large on the tensile side where the axial stress is rather small. This tendency is predominant particularly for the ductile iron pipelines with the K and A-joints. In Fig. 12 (c), the relative joint motion has large values at both ends of the line, which result from the boundary conditions of analytical models and should be disregarded. These phenomena will be shown in the distributions of the response values, and their treatment will be the same.

[2] *Bent pipes, angle of bent pipes, and interval of two bent pipes*

Fig. 13 shows the distributions of the response values for Model-II. The bending stress, which does not excel in straight pipes, has large values at the bent sections and are indicated by arrow signs. The maximum response values for Models I~IV, under the same condition of the earthquake intensity, are listed in Table 7. In Table 7, the maximum relative joint motion and the maximum axial stress have the same value in Models I~IV, because these maximum values take place at the straight part of the pipelines. On the other hand, the rotational joint motion and the bending stress excel in the bent pipes, and the maximum total fiber stress is larger in the bent pipes than in the straight pipes. In the case of Model IV, the maximum rotational joint motion amounts to  $1.35^\circ$ . Even this value is smaller than the allowance rotational joint motion ( $=2.17^\circ$  for  $\phi_d=800$ ) for leakage (6), the relative joint displacement at this point by the rotational motion reaches about 1.9 cm, using the following equation:

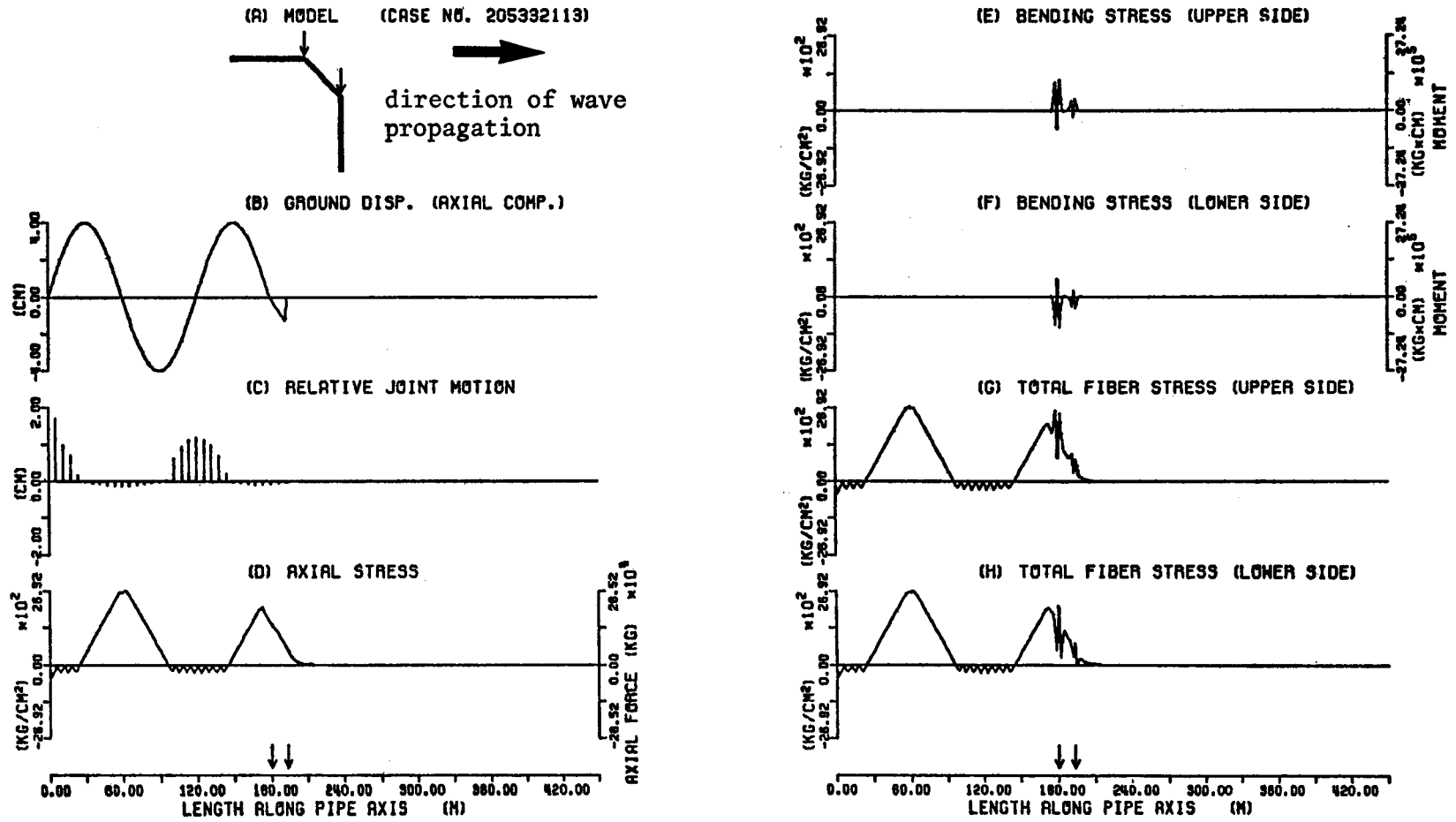
$$\delta_r = \phi_d \sin \theta_r \quad (30)$$

where  $\theta_r$  is the rotational joint motion in radian. The total relative joint displacement  $\delta_t$  at this point is estimated by adding the longitudinal relative joint displacement  $\delta_l$  ( $=0.9$  cm) to  $\delta_r$  as



wave length	120 m	bent angle	0°
disp. amplitude	4 cm	soil spring	750 kg/cm <sup>2</sup>
diameter	800 cm	interval between 2 bent pipes	m

Fig. 12. Distributions of Response Values (Model-I).



wave length	120 m	bent angle	45 °
disp. amplitude	4 cm	soil spring	750 kg/cm <sup>2</sup>
diameter	400 cm	interval between	12 m
		2 bent pipes	

Fig. 13. Distributions of Response Values (Model-II).

Table 7. Maximum Response Values.

	model-I	model-II	model-III	model-IV
relative joint motion (cm)	1.23	1.23	1.23	1.23
rotational joint motion (°)	0	0.32	0.29	1.35
axial stress (kg/cm <sup>2</sup> )	1234	1227	1227	1227
bending stress (kg/cm <sup>2</sup> )	0	601	684	635
shear stress (kg/cm <sup>2</sup> )	0	182	202	122
total fiber stress (kg/cm <sup>2</sup> )	1234	1481	1633	1407

( $L=120$  m,  $U_m=4$  cm,  $k_s=750$  kg/cm,  $\phi_d=800$  mm, angle of bent pipe=45°)

$$\delta_t = \delta_r + \delta_i \tag{31}$$

and  $\delta_i$  gets to  $\delta_i=2.8$  cm. One of the reasons for this large relative joint motion is thought to be that the vertical sections of the pipelines are compelled to the ground motions and that the pipes move discontinuously at the curved sections where the direction of the pipelines change.

Fig. 14 shows the effect of the bent angles on the response values in the case of Model-II with two bent angles of 45° and 22½°. The maximum relative joint motion and the maximum axial stress do not differ in these two bent angles, because they occur at the straight part of pipelines. On the other hand, the total fiber stress is a little larger in the case of the 22½° bent pipe than for the 45° bent pipe. Even the bending stress is contrary. The reason for this result is that the axial stress still excels in the bent pipes, and it is larger in 22½° pipes than in 45° pipes.

Fig. 15 shows the effect of the interval between two bent pipes on the response values for Models-II, III, and IV. As for the maximum relative joint motion, it

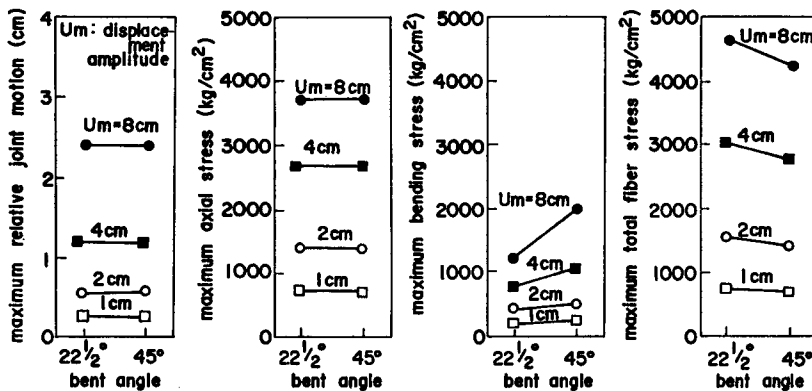


Fig. 14. Effect of Bent Angle on Maximum Response Values (Model-II,  $\phi_d=400$  mm,  $k_s=750$  kg/cm<sup>2</sup>).

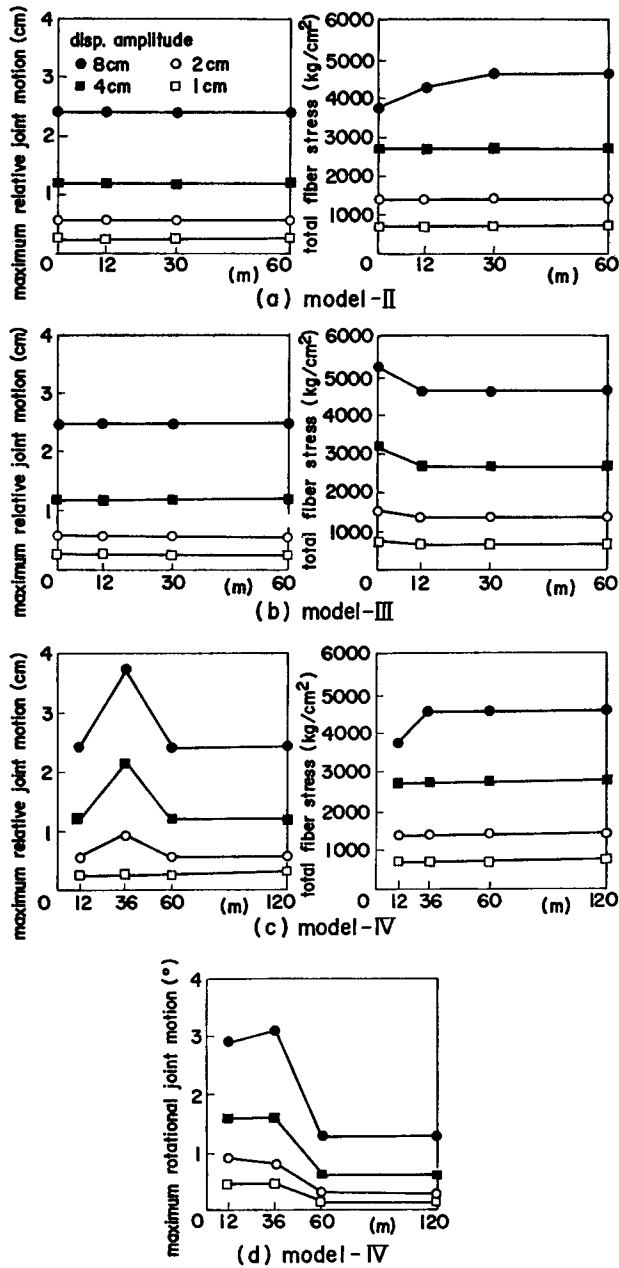


Fig. 15. Effect of Interval between Two Bent Pipes on Maximum Response Values ( $\phi_d=400$  mm,  $k_s=750$  kg/cm).

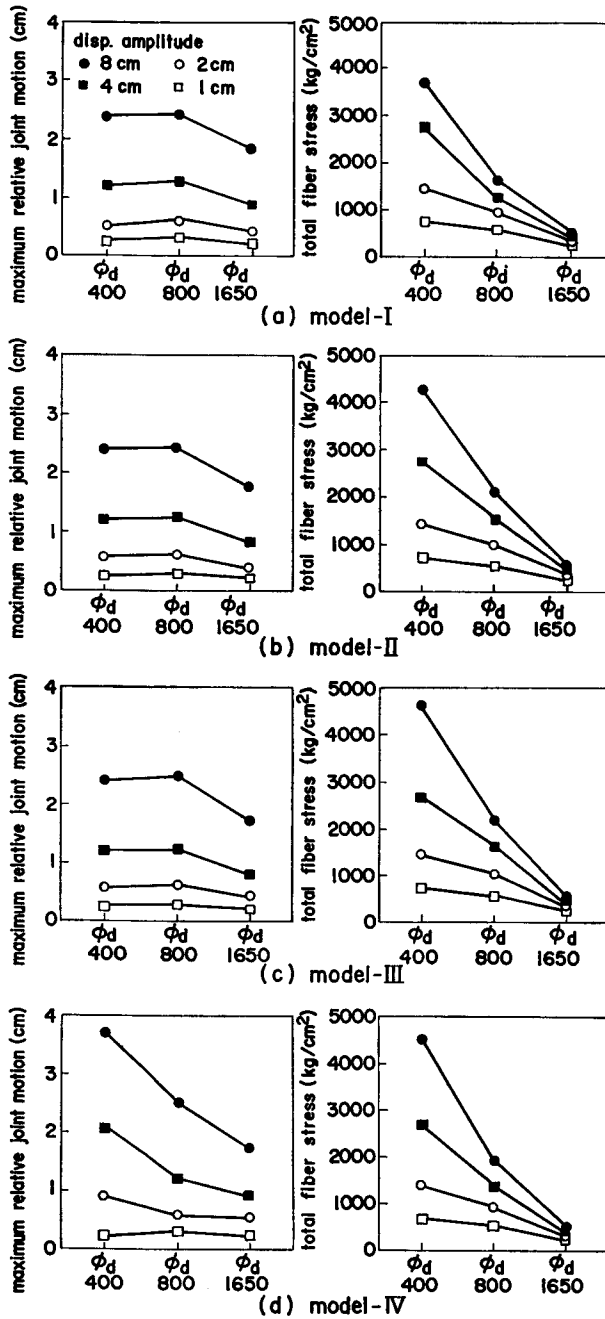


Fig. 16. Effect of Diameter of Pipes on Maximum Response Values ( $k_s = 750$  kg/cm).

does not depend on the interval between two bent pipes except for the case of the interval 36 m of Model-IV. Only this special response value occurs at the bent pipe. The total fiber stress does not depend very much on the interval between two bent pipes through these models. In the cases where the interval equals 0 m for these models, even a type of which does not exist in the actual systems, the total fiber stress differs from the ordinary types.

[3] *Diameter of pipes*

Fig. 16 shows the response values of Models-I~IV for the diameters of  $\phi_d=400$ ,  $\phi_d=800$ , and  $\phi_d=1650$  mm. As for the relative joint motion, it is proportional to the displacement amplitude, and only in the case where the diameter  $\phi_d=1650$  it is smaller than in other cases. This difference results from the unit length of the pipes. Namely, the relative joint motion depends on the number of joints included in a half length of the wave. These results coincide with the experimental results of Miyamoto, Hojyo, and Kosho (9), and also with the views of Toki (20), Takada and Takahashi (17) for the estimation of the joint motions. On the other hand, the total fiber stress depends on the diameter of the pipes. In the case of the large diameter, the stiffness of the pipes is relatively large and slippage between the pipe and the surrounding soil occurs easily: i.e., the axial stress decreases.

From the above results, it may be said that the relative joint motion depends on the unit length of the pipes, and that the total fiber stress depends on the stiffness of the pipes. In other words, it depends on the diameter of pipes.

[4] *Soil springs*

Fig. 17 shows the response values of Models-I~IV for the soil springs of  $k_s=300$ , 750, and 1200 kg/cm<sup>2</sup>. The maximum relative joint motion does not differ mostly in soil springs, because it occurs in the tensile region of the ground motions where the joint moves easily and slippage does not occur. On the other hand, the total fiber stress depends on the soil springs especially in cases of large displacement amplitudes. In the case of a large displacement amplitude such as  $u_m=4$  and 8 cm, slippage occurs when the soil spring is small, and it causes a large difference on the axial stress between for the large and small soil springs.

[5] *Wave length and amplitude of input displacement*

Figs. 18 and 19 show the response values of Model-I for the wave lengths of 120 m and 600 m for the same displacement amplitude. In the case of the large wave length (Fig. 19), the distribution of the axial stress represents a sinusoidal curve which is the shape of the input ground displacement, and the response values are smaller than in cases with a small wave length (Fig. 18). These differences in the

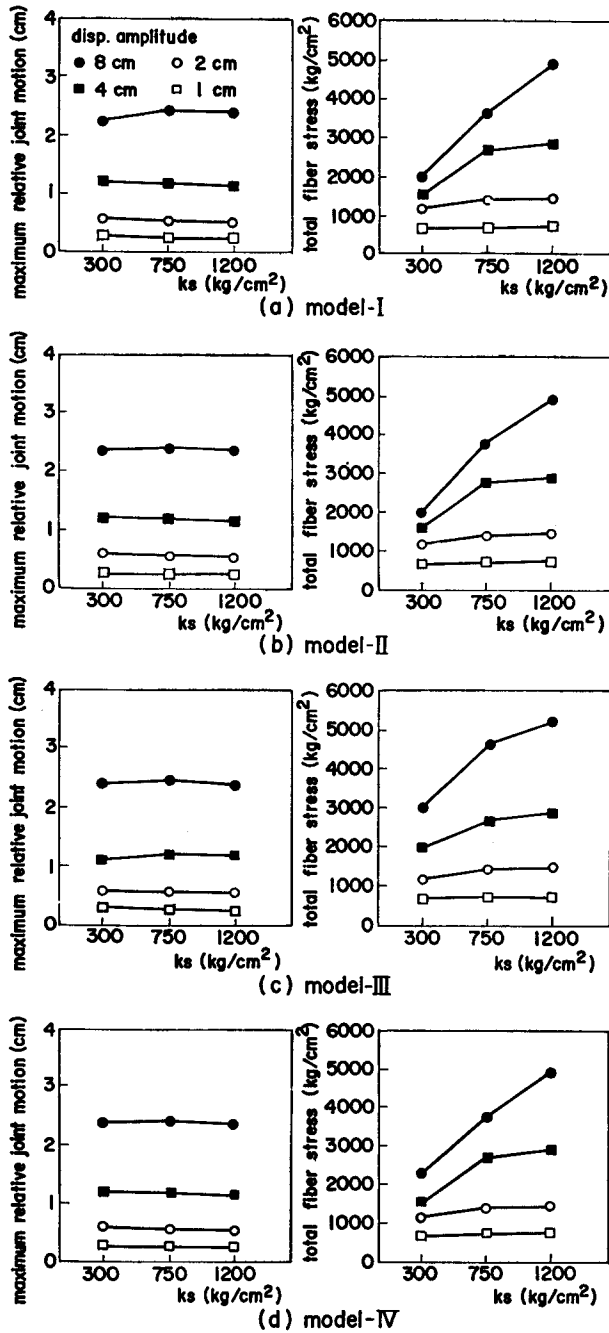


Fig. 17. Effect of Soil Spring on Maximum Response Values ( $\phi_d=400$  mm).



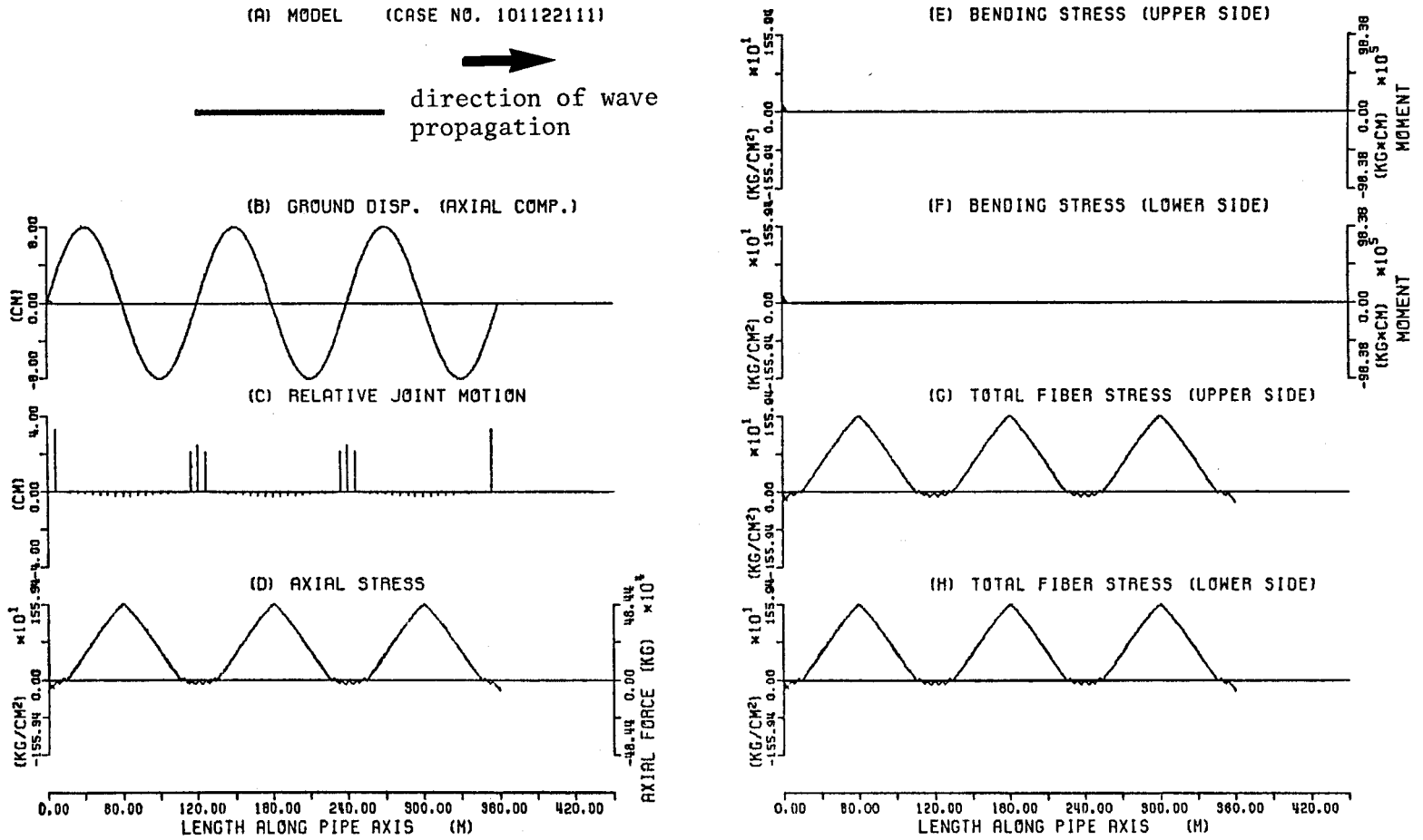
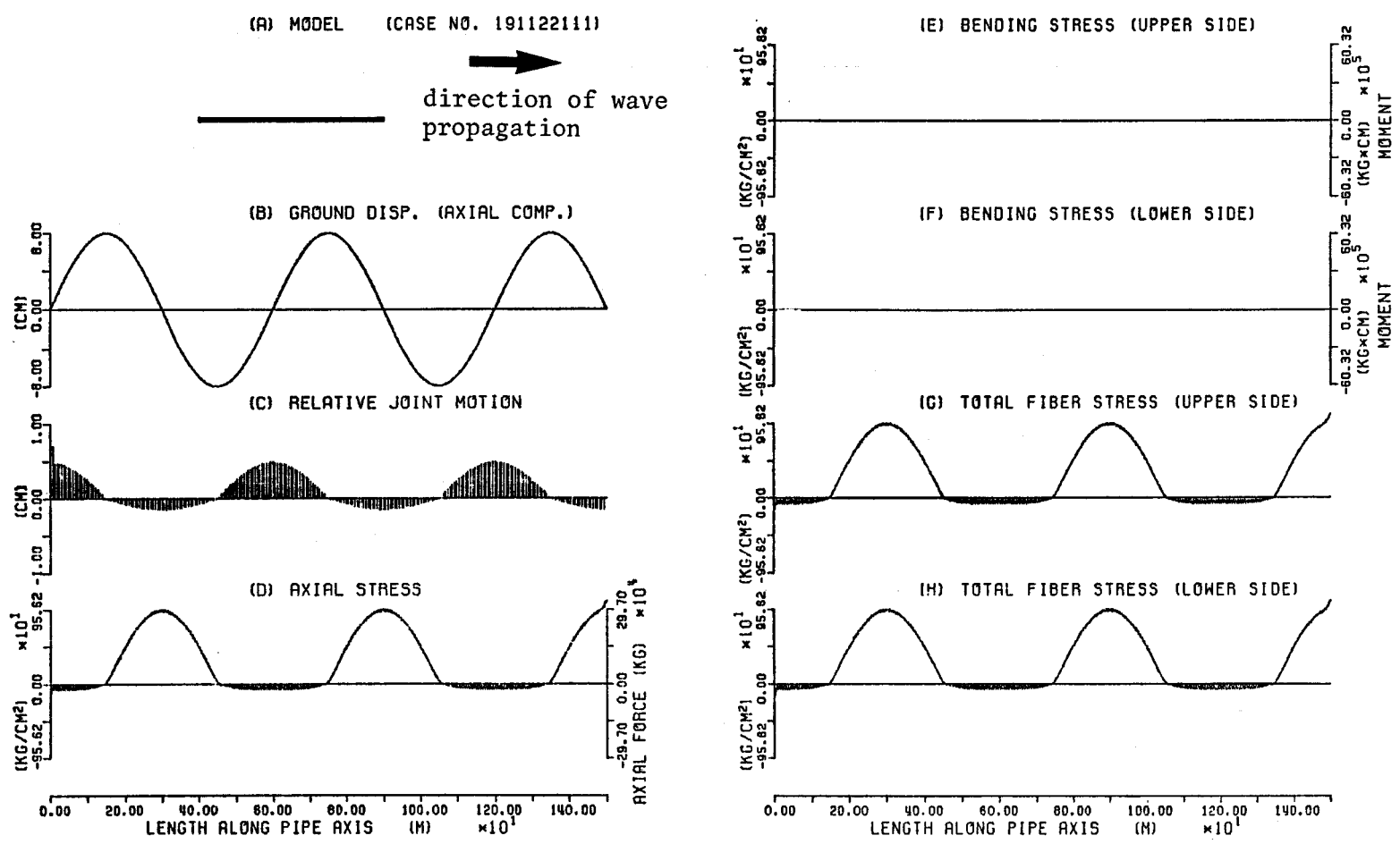


Fig. 18. Distributions of Response Values (Model-I).



wave length	600 m	bent angle	°
disp. amplitude	4 cm	soil spring	750 kg/cm <sup>2</sup>
diameter	800 mm	interval between	m
		2 bent pipes	

Fig. 19. Distributions of Response Values (Model-I).

shapes of the response distributions are concerned with the slippage between pipes and surrounding soil. In Fig. 18, slippage occurs mainly in the compression regions of the pipes because of the large ground strain.

Table 8 shows the maximum response values for each displacement amplitude in Models-I~IV. It may be observed that the ratio of increase for the relative

Table 8. Maximum Response Values for Each Displacement Amplitude.

model	displacement amplitude	relative joint motion		rotational joint motion		axial stress		bending stress		total fiber stress	
		(cm)	ratio	(°)	ratio	(kg/cm <sup>2</sup> )	ratio	(kg/cm <sup>2</sup> )	ratio	(kg/cm <sup>2</sup> )	ratio
(I)	1	0.26	1.0	0	—	706	1.0	0	—	706	1.0
	2	0.57	2.19	0	—	1413	2.00	0	—	1413	2.00
	4	1.19	4.58	0	—	2680	3.80	0	—	2680	3.80
	8	2.42	9.31	0	—	3684	5.22	0	—	3684	5.22
(II)	1	0.26	1.0	0.10	1.0	708	1.0	236	1.0	708	1.0
	2	0.57	2.19	0.20	2.00	1416	2.00	506	2.14	1416	2.00
	4	1.19	4.58	0.44	4.40	2692	3.80	1088	4.61	2692	3.80
	8	2.42	9.31	0.85	8.50	3735	5.28	2023	8.57	4255	6.01
(III)	1	0.26	1.0	0.10	1.0	712	1.0	239	1.0	712	1.0
	2	0.56	2.15	0.20	2.00	1423	2.00	512	2.14	1423	2.00
	4	1.19	4.58	0.43	4.30	2704	3.80	1108	4.64	2704	3.80
	8	2.46	9.46	0.78	7.80	3768	5.29	2127	8.90	4616	6.48
(IV)	1	0.26	1.0	0.47	1.0	709	1.0	280	1.0	709	1.0
	2	0.92	3.54	0.82	1.74	1418	2.00	523	1.87	1418	2.00
	4	2.17	8.35	1.57	3.34	2694	3.80	1128	4.03	2694	3.80
	8	3.75	14.42	3.08	6.55	3742	5.28	2368	8.46	4532	6.39

( $L=120$  m,  $\phi_d=400$  mm,  $k_s=750$  kg/cm<sup>2</sup>, angle of bent pipe=45°)

joint motion is larger than that for the input displacement amplitudes. On the other hand, it may be observed that the ratio of increase for the total fiber stress is smaller, especially in cases of large displacement amplitudes because of the effect of the slippage. However, it should be remarked that the ratio of increase for the total fiber stress in Models-II~IV, which have bent pipes, is not so small even in cases of large displacement amplitudes compared with that in Model-I.

[6] *Angle of incidence and phase of input displacement*

The angle of incidence affects only the apparent wave length and the ground displacement in the axial direction. Moreover, the phase of the input displacement has no meaning for the straight part of the pipelines. Hence, these effects are examined for Model-II as a typical model including bent sections.

Fig. 20 shows the effect of the angle of incidence on the maximum response values. The angle of incidence is examined for the three cases of (1) 0°, (2) 45°, (3) 90° to the section (b) between two bent pipes. As for the relative joint motion, the peak value occurs in the straight parts (a) or (b), and it is largest in the case of the angle (2) 45° for each displacement amplitude, because the ground displacement in the axial direction is largest for the straight part (a) in this angle of incidence. The maximum total fiber stress is influenced complexly by the angle of

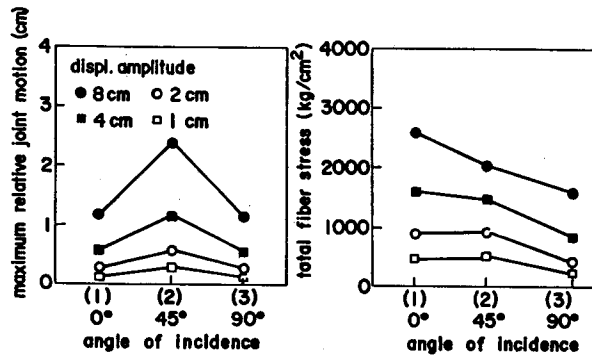
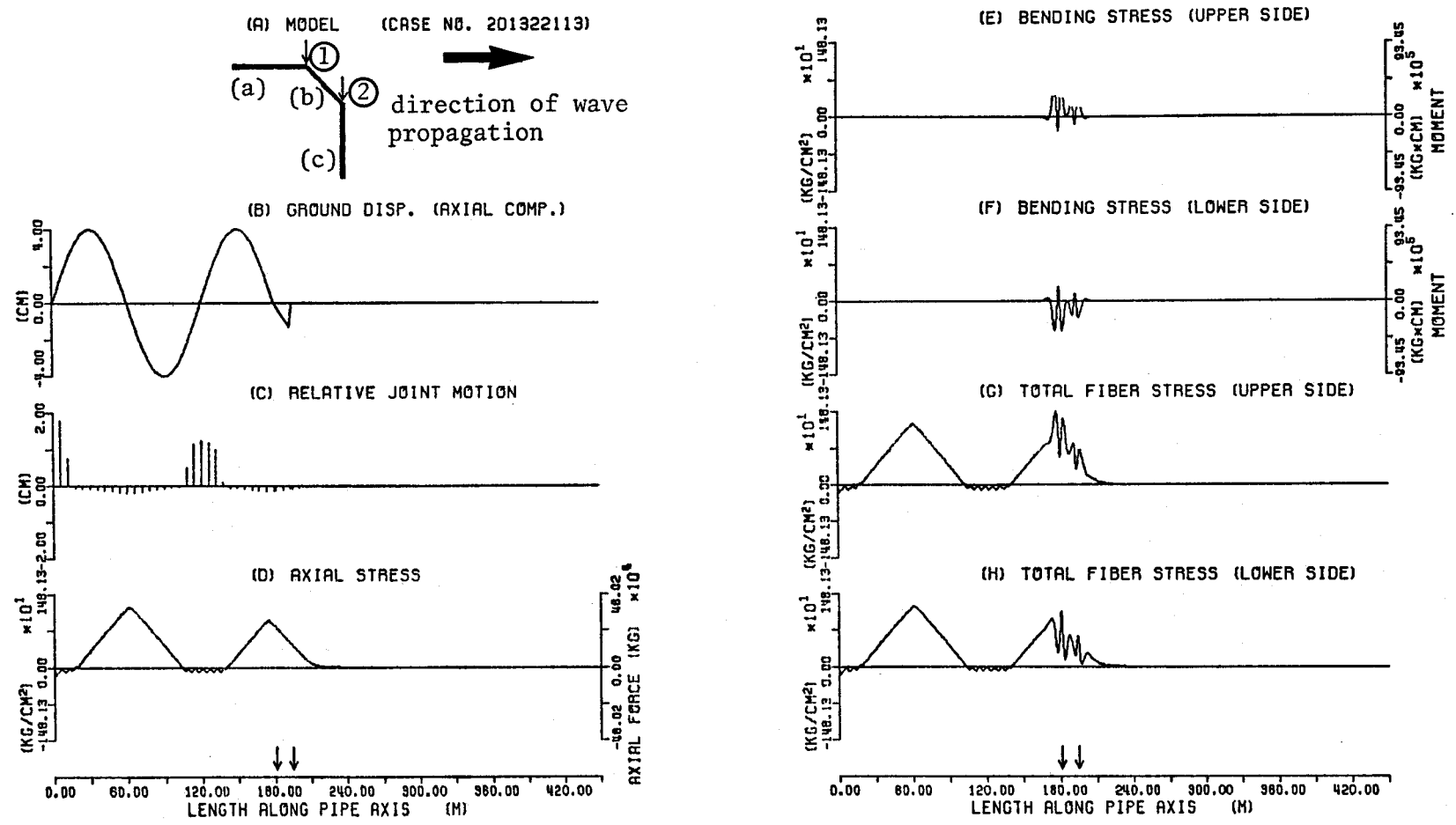


Fig. 20. Effect of Angle of Incidence on Maximum Response Values (Model-II,  $\phi_d=800$  mm,  $k_s=750$  kg/cm).

incidence and the displacement amplitude. In the cases of small amplitudes, where slippage does not occur, the maximum total fiber stress occurs at the straight part (a) or (c), and it is largest in the angle of incidence (2) 45°. However, in cases of large displacement amplitudes, where slippage occurs, the maximum total fiber stress occurs at the bent sections, and it is largest in the angle of incidence (1) 0°.

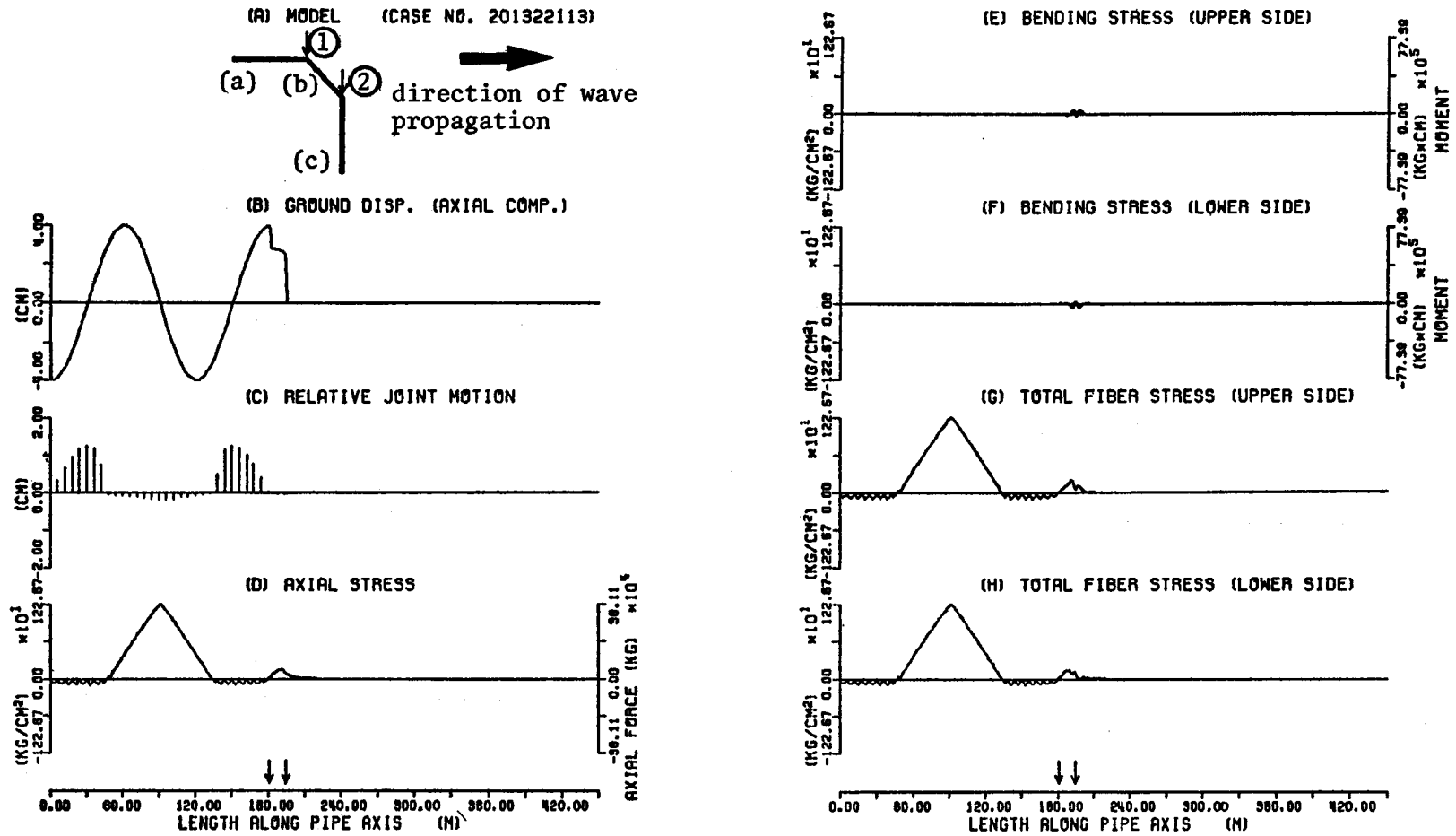
The effect of the phase of the input displacement on the response values is shown in Figs. 21~24. In these figures, it may be observed that only the bending stress at the bent pipes is effected by the phase, and it is in proportion to the axial stress at the same point. In the case of phase (1), where the compression strain takes the maximum value at the bent pipe ①, the maximum total fiber stress occurs at this bent pipe.

Fig. 25(a)~(d) shows the maximum response values of Models I~IV versus



wave length	120 m	bent angle	45 °
disp. amplitude	4 cm	soil spring	750 kg/cm <sup>2</sup>
diameter	800 mm	interval between	12 m
			2 bent pipes

Fig. 21. Distributions of Response Values (Model-II).



wave length	120 m	bent angle	45 °
disp. amplitude	4 cm	soil spring	750 kg/cm <sup>2</sup>
diameter	800 mm	interval between	12 m
		2 bent pipes	

Fig. 22. Distributions of Response Values (Model-II).



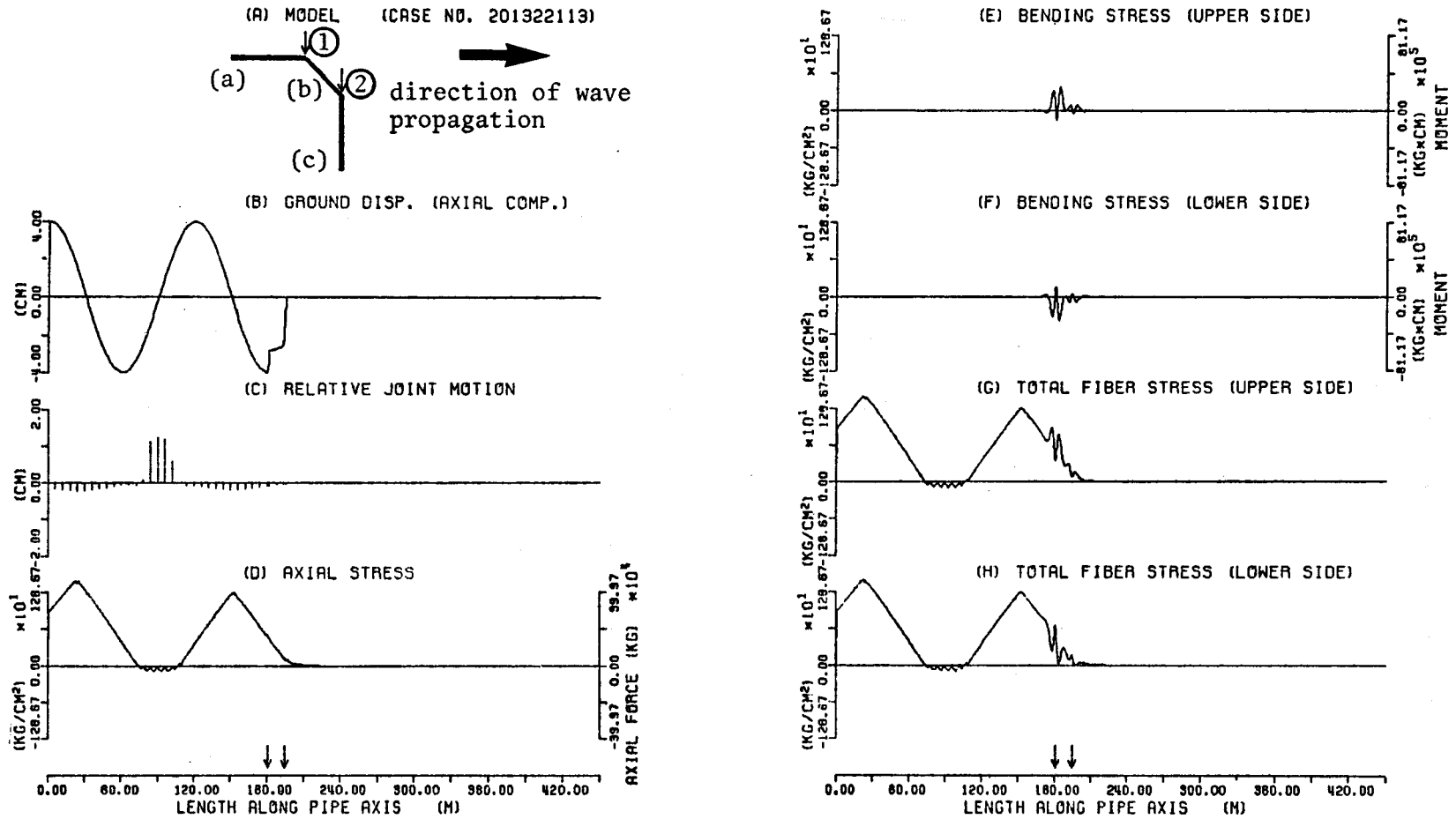


Fig. 24. Distributions of Response Values (Model-II).



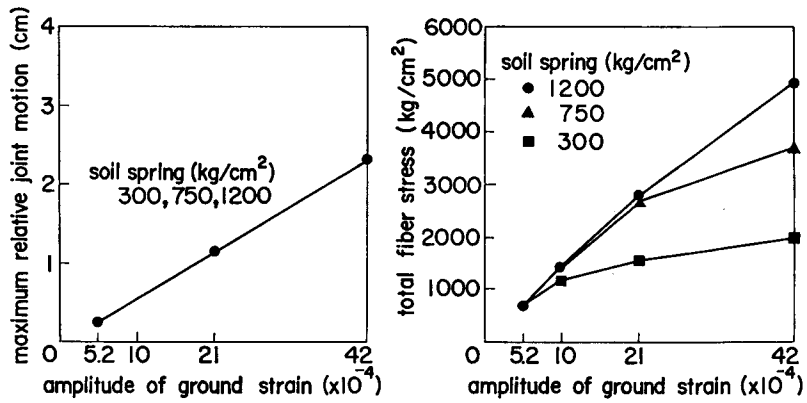


Fig. 25(a). Maximum Response Values versus Amplitude of Ground Strain (Model-I,  $\phi_d=400$  mm).

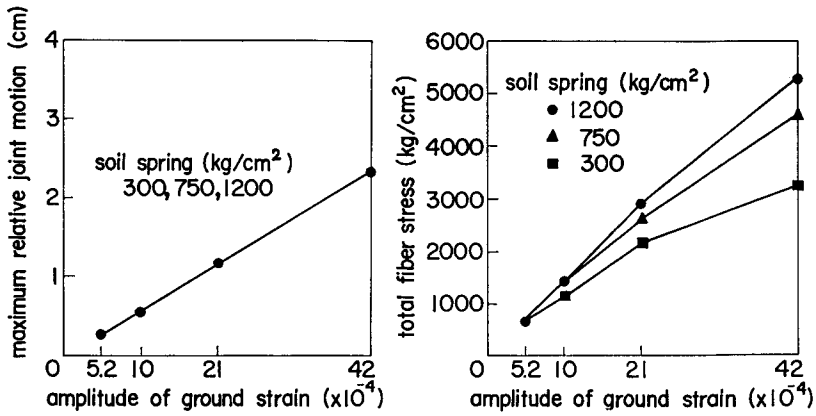


Fig. 25(b). Maximum Response Values versus Amplitude of Ground Strain (Model-II,  $\phi_d=400$  mm).

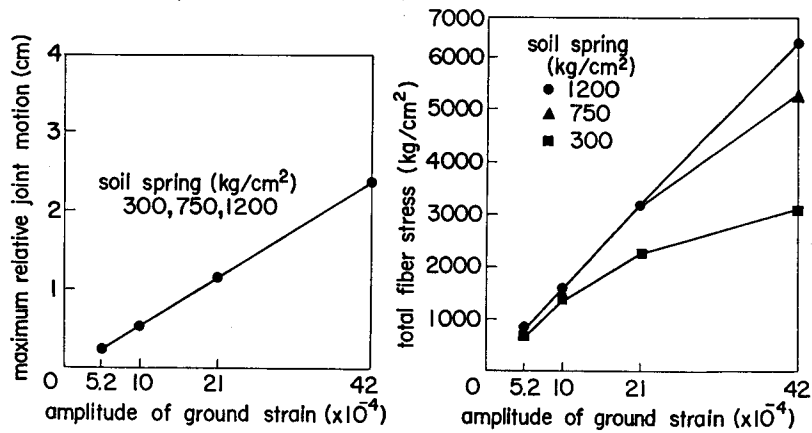


Fig. 25(c). Maximum Response Values versus Amplitude of Ground Strain (Model-III,  $\phi_d=400$  mm).

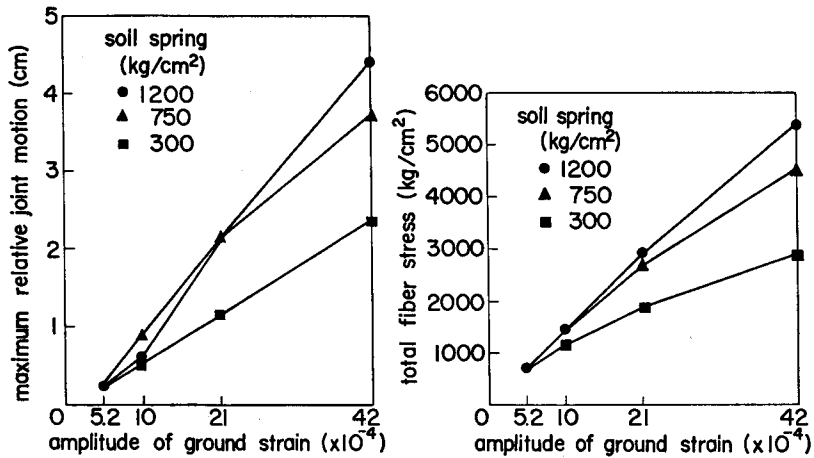


Fig. 25(d). Maximum Response Values versus Amplitude of Ground Strain (Model-IV,  $\phi_d=400$  mm).

the amplitude of ground strain for the three values of the soil springs. In these figures, it may be observed that the relative joint motion is completely in proportion to the ground strain, and it does not depend on the soil spring, except for the case of Model-IV. Also, the maximum total fiber stress depends mostly on the ground strain and the soil spring. Further, it can be said that the decrease of the stress caused by slippage is not so remarkable in Models-II~IV, which have the bent pipes, as in Model-I.

From the above discussion on the response characteristics of joint-connected buried pipelines, the following articles are summarized.

(1) *Response characteristics of joint-connected pipelines*

The most prominent response characteristics of joint-connected pipelines is that the joint can absorb the ground strain on the side where the joint is movable, and that the axial stress scarcely occurs in the pipes when the joint slides. In the cases of the ductile A and K-joints, which are commonly used in the actual systems, their response characteristics in the tensile and compressive sides are quite different. Accordingly, the response characteristics of pipelines which consist of these kinds of joints are rather complicated, as discussed above. These results indicate that the ductile S-joint, which can move both the tensile and compressive sides, will absorb both the tensile and compressive ground strains along the pipes, and axial stress will not occur mostly. For this type of joint, the displacement capacity of the joints will be the sole parameter for the assessment of the reliability of the pipelines as regards the earthquake ground motion.

(2) *Response characteristics of pipelines including bent sections*

From the above discussions, it can be recognized that the response values at the bent sections are strongly effected by the phase of the input ground motion, and they surpass the straight part of pipelines. It is also recognized that in the case of Model-IV, which is a typical type where the pipeline passes under rivers, buried structures, etc., the rotational joint motion receives considerably large values for some special structural and input conditions.

In the above figures which show the response values, it is sometimes recognized that the total fiber stress surpasses the tensile strength of the ductile iron (more than 4000 kg/cm<sup>2</sup>) for the displacement amplitude  $u_m=8$  cm. The value  $u_m=8$  cm, however, is regarded to be considerably large with reference to the attenuation equation of the ground displacement by Goto, Kameda, and Sugito (2). This large amplitude is applied to examine the intensity level of the ground strain which causes the breakage of pipes.

#### 4. Conclusions

The major results of this study may be summarized as follows.

- (1) The details of the structures and materials along the trunk routes of the Kyoto City Water Supply System have been thoroughly examined to establish analytical models of pipelines which are commonly used in the actual lifeline systems.
- (2) From the survey on the actual lifeline systems, significant information such as the structural characteristics of joints, the structural forms at bent sections, the percentage of the angles in bent pipes, etc. has been obtained.
- (3) Non-linear response analysis of joint-connected buried pipelines has been carried out with various values of structural and input ground motion parameters, using the transfer matrix method.
- (4) The effects of the structural and input ground motion parameters on the response behavior of buried pipelines have been examined in terms of the maximum total fiber stress for straight and bent pipes, and the relative and rotational joint motions for bent pipes.

#### Acknowledgements

The authors would like to express their deep appreciation to the staffs of the Kyoto City Water Supply System for the detailed data on the trunk routes of the system, and also to the staffs of the Pipe Research Department at Kubota LTD, for the data on the structural characteristics of pipe joints. Further, they would like

to acknowledge the assistance of the students of their laboratory at Kyoto University in the investigation and the arrangement of the data on the Kyoto City Water Supply System. Also, they would like to express their appreciation to Professor Shiro Takada of Kobe University for the offer of the computer program for the response analysis. The numerical computation for this study has been performed on the FACOM M-200 computer system of the Data Processing Center, Kyoto University.

#### References

- 1) Kuribayashi, E., Iwasaki, T., Kawashima, K., and Miyata, T., "Experimental Study on Dynamic Relative Displacement and Resistant Strength between Buried Pipes and Soil," Transactions of Public Works Research Institute, Ministry of Construction, No. 1266, July 1977, (in Japanese).
- 2) Goto, H., Kameda, H., and Sugito, M., "Use of N-value Profiles for Estimation of Site-Dependent Earthquake Motions," Proc. of JSCE, No. 317, Jan. 1982, (in Japanese).
- 3) Hall, W.J. and Newmark, N.M., "Seismic Design Criteria for Pipelines and Facilities," Current State of Knowledge of Lifeline Earthquake Engineering, ASCE, Aug. 1977. pp. 18-34.
- 4) Japan Society of Water Supply Institution, "Guide and Commentary for Earthquake Resistant Construction Code of Water Supply Facilities," 1979.
- 5) Kamiyama, M., "Stress and Strain in Ground During Earthquake," Proc. of JSCE, No. 250, June 1976, pp. 9-23, (in Japanese).
- 6) Kubota, LTD., "Handbook of Ductile Iron Pipe," 1976, (in Japanese).
- 7) Kyoto City (General Affairs Bureau), "Boring Data in Kyoto City," 1979.
- 8) Miyajima, N. and Miyauchi, J., "Stresses in Buried Pipes during Earthquake Based on Static Friction," Proc. of Symposium on Buried Pipelines, Japan Society of Soil Mechanics and Foundation Engineering, Oct. 1975, pp. 57-60, (in Japanese).
- 9) Miyamoto, H., Hojyo, S., and Kosho, K., "Vibration Tests of Buried Pipes for Estimation of Its Behavior during Earthquakes," Kubota Technical Report, Vol/1, No. 2, Dec. 1976, pp. 126-153, (in Japanese).
- 10) Muleski, G.E., Ariman, T., and Aumen, C.P., "A Shell Model of a Buried Pipe in a Seismic Environment," Journal of Pressure Vessel Technology, Vol. 101, Feb. 1979, pp. 44-50.
- 11) Naruoka, M. and Toda, Y., "Transfer Matrix Method," Baifu-kan, 1970, (in Japanese).
- 12) Saionji, S., Taguchi, M., Tsuzuki, K., and Tabata, H., "Stress at Bent Section of Buried Pipes during Earthquakes," Proc. of the 5th Japan Earthquake Engineering, Nov. 1978, pp. 929-936, (in Japanese).
- 13) Sakurai, A. and Takahashi, T., "Dynamic Stresses of Underground Pipelines during Earthquakes" Proc. of the 4th World Conference on Earthquake Engineering, Santiago, Vol. II, pp. 81-95, 1969.
- 14) Shinozuka, M. and Koike, T., "Estimation of Structural Strains in Underground Lifeline Pipes," Lifeline Earthquake Engineering-Buried Pipelines, Seismic Risk and Instrumentation, ASME, June 1979, pp. 31-48.
- 15) Takada, S. and Nagao, S., "Dynamic Frictional Forces and Efficiency of Joint Parts for Aseismic Strength of Buried Pipelines," Proc. of the U.S.-Japan Seminar on Earthquake Engineering with Emphasis on Lifeline Systems, Tokyo, Nov. 1976, pp. 211-222.
- 16) Takada, S., "Seismic Response Analysis of Buried PVC and Ductile Iron Pipelines," The 1980 Pressure Vessels and Piping Conference, ASME, Aug. 1980, pp. 23-32.
- 17) Takada, S. and Takahashi, S., "On the Estimation for Relative Displacement at Joint of Buried Pipes during Earthquakes," Proc. of the 34th Annual Convension, JSCE, Oct. 1979, pp. 352-353, (in Japanese).

- 18) Toki, K., "Influence of Seismic Ground Motion from Earthquake Records," Proc. of JSCE, Vol. 207, Nov. 1972, pp. 25-36, (in Japanese).
- 19) Toki, K., "Estimation of Seismic Damage of Water System," Disaster Prevention Research Institute Annuals, No. 22B-2, pp. 1-23, 1979, (in Japanese).
- 20) Toki, K., "Estimation of Seismic Damage of Water Pipelines in Osaka City," Bosai-10, Osaka City Disaster Prevention Committee, Oct. 1973, (in Japanese).
- 21) Ukai, K. and Yamaguchi, H., "Theoretical Research for Behavior of Buried Pipes during Earthquakes," Proc. of the 5th Japan Earthquake Engineering, Nov. 1978, pp. 433-436, (in Japanese).
- 22) Wang, L.R.-L., "Seismic Analysis and Design of Buried Pipelines," Proc. of International Conference on Engineering for Protection from Natural Disasters, Bangkok, Jan. 1980, pp. 71-83.

### Appendix A.

A1. The functions  $B_1(x) \sim B_6(x)$  and  $D_1(x) \sim D_6(x)$  in Eqs. (15)~(20) are represented as follows.

$$B_1(x) = \cos \beta_1 x \cosh \beta_1 x \quad (\text{A-1})$$

$$B_2(x) = \sin \beta_1 x \sinh \beta_1 x \quad (\text{A-2})$$

$$B_3(x) = \cos \beta_1 x \sinh \beta_1 x + \sin \beta_1 x \cosh \beta_1 x \quad (\text{A-3})$$

$$B_4(x) = \cos \beta_1 x \sinh \beta_1 x - \sin \beta_1 x \cosh \beta_1 x \quad (\text{A-4})$$

$$B_5(x) = \cosh \beta_2 x \quad (\text{A-5})$$

$$B_6(x) = \sinh \beta_2 x \quad (\text{A-6})$$

$$D_1(x) = -v_0(0) B_1(x) - \frac{v_0'(0)}{2\beta_1} B_3(x) - \frac{v_0''(0)}{2\beta_1^2} B_2(x) + \frac{v_0'''(0)}{4\beta_1^3} B_4(x) + v_0(x) \quad (\text{A-7})$$

$$D_2(x) = v_0(0) \beta_1 \cdot B_4(x) + v_0'(0) B_1(x) + \frac{v_0''(0)}{2\beta_1} B_3(x) + \frac{v_0'''(0)}{2\beta_1^2} B_2(x) - v_0'(x) \quad (\text{A-8})$$

$$D_3(x) = 2v_0(0) EI \beta_1^2 \cdot B_2(x) - v_0'(0) EI \beta_1 \cdot B_4(x) \\ - v_0''(0) EIB_1(x) - \frac{v_0'''(0) EI}{2\beta_1} B_3(x) + EIv_0'''(x) \quad (\text{A-9})$$

$$D_4(x) = 2v_0(0) EI \beta_1^3 \cdot B_3(x) + 2v_0'(0) EI \beta_1^2 \cdot B_2(x) \\ - v_0''(0) EI \beta_1 \cdot B_1(x) - v_0'''(0) EIB_1(x) + EIv_0'''(x) \quad (\text{A-10})$$

$$D_5(x) = -u_0(0) B_5(x) - \frac{u_0'(0) B_6(x)}{\beta_2} + u_0(x) \quad (\text{A-11})$$

$$D_6(x) = u_0(0) EA \beta_2 \cdot B_6(x) + u_0'(0) EAB_5(x) - EAu_0'(x) \quad (\text{A-12})$$

A2. The field matrix  $\mathbf{F}$  in Eq. (21) and the point matrix  $\mathbf{P}$  in Eq. (24) at the joints of straight and bent sections are represented as follows:

$$\mathbf{F} = \begin{pmatrix} B_5(l) & 0 & 0 & -\frac{B_6(l)}{EA\beta_2} & 0 & 0 & D_5(l) \\ 0 & B_1(l) & -\frac{B_3(l)}{2\beta_1} & 0 & \frac{B_2(l)}{2\beta_1^2 EI} & -\frac{B_4(l)}{4\beta_1^3 EI} & D_1(l) \\ 0 & -\beta_1 B_4(l) & B_1(l) & 0 & -\frac{B_3(l)}{2\beta_1 EI} & -\frac{B_2(l)}{2\beta_1^2 EI} & D_2(l) \\ -EA\beta_2 B_6(l) & 0 & 0 & B_5(l) & 0 & 0 & D_6(l) \\ 0 & -2EI\beta_1^2 B_2(l) & -\beta_1 EIB_4(l) & 0 & B_1(l) & \frac{B_3(l)}{2\beta_1} & D_3(l) \\ 0 & -2EI\beta_1^3 B_3(l) & 2\beta_1^2 EIB_2(l) & 0 & \beta_1 B_4(l) & B_1(l) & D_4(l) \\ 0 & 0 & 0 & 0 & 0 & 0 & 1 \end{pmatrix} \quad (\text{A-13})$$

for the straight section:

$$\mathbf{P} = \begin{pmatrix} 1 & 0 & 0 & -\frac{1}{k_T} & 0 & 0 & 0 \\ 0 & 1 & 0 & 0 & 0 & 0 & 0 \\ 0 & 0 & 1 & 0 & -\frac{1}{k_R} & 0 & 0 \\ 0 & 0 & 0 & 1 & 0 & 0 & 0 \\ 0 & 0 & 0 & 0 & 1 & 0 & 0 \\ 0 & 0 & 0 & 0 & 0 & 1 & 0 \\ 0 & 0 & 0 & 0 & 0 & 0 & 1 \end{pmatrix} \quad (\text{A-14})$$

for the bent section:

$$\mathbf{P} = \begin{pmatrix} \cos \alpha & \sin \alpha & 0 & -\frac{\cos \alpha}{k_T} & 0 & \frac{\sin \alpha}{k_T} & 0 \\ -\sin \alpha & \cos \alpha & 0 & 0 & 0 & 0 & 0 \\ 0 & 0 & 1 & 0 & -\frac{1}{k_R} & 0 & 0 \\ 0 & 0 & 0 & \cos \alpha & 0 & \sin \alpha & 0 \\ 0 & 0 & 0 & 0 & 1 & 0 & 0 \\ 0 & 0 & 0 & -\sin \alpha & 0 & \cos \alpha & 0 \\ 0 & 0 & 0 & 0 & 0 & 0 & 1 \end{pmatrix} \quad (\text{A-15})$$

**Appendix B. Notations**

- $A$  = cross sectional area of the pipe (cm<sup>2</sup>)  
 $\mathbf{A}_1^L$  = initial matrix  
 $C_1 \sim C_6$  = constants of integration  
 $c$  = apparent wave speed along the axial direction (cm/sec)  
 $d_s$  = relative displacement at which slippage between pipe and soil occurs (cm)  
 $E$  = Young's modulus of pipe material (kg/cm<sup>2</sup>)  
 $\mathbf{F}$  = field matrix  
 $G_s$  = shear modulus of soil (kg/cm<sup>2</sup>)  
 $g$  = acceleration of gravity (=980 cm/sec<sup>2</sup>)  
 $I$  = geometrical moment of inertia of pipe (cm<sup>4</sup>)  
 $K_{g1}$  = soil spring constant for unit length in axial direction of pipe (kg/cm<sup>2</sup>)  
 $K_{g2}$  = soil spring constant for unit length in transverse direction of pipe (kg/cm<sup>2</sup>)  
 $k_{g1}$  = constant used for estimation of soil spring constant  $K_{g1}$   
 $k_{g2}$  = constant used for estimation of soil spring constant  $K_{g2}$   
 $k_{sx}$  = equivalent spring constant for longitudinal motion to reflect soil-structure interaction (kg/cm<sup>2</sup>)  
 $k_{sy}$  = equivalent spring constant for transverse motion to reflect soil-structure interaction (kg/cm<sup>2</sup>)  
 $k_T$  = translational (longitudinal) spring of joint (kg/cm)  
 $k_R$  = rotational spring of joint (kg·cm/°)  
 $L$  = wave length (m)  
 $l$  = unit length of pipe (cm)  
 $M$  = bending moment of pipe (kg·cm)  
 $M^L$  = bending moment at the left boundary of pipeline (kg·cm)  
 $N$  = axial force of pipe (kg)  
 $N^L$  = axial force at the left boundary of pipeline (kg)  
 $\mathbf{P}$  = point matrix  
 $Q$  = shear force of pipe (kg)  
 $Q^L$  = shear force at the left boundary of pipeline (kg)  
 $\mathbf{R}$  = boundary matrix at the left side of pipeline  
 $\mathbf{R}'$  = boundary matrix at the right side of pipeline  
 $t$  = time variable  
 $u$  = longitudinal displacement of pipe (cm)  
 $u^L$  = longitudinal displacement at the left boundary of pipeline (cm)  
 $u_0(x)$  = particular solution for longitudinal equation of motion  
 $u_m$  = displacement amplitude of free field (cm)

- $u_{s_x}$  = longitudinal displacement of free field (cm)  
 $u_{s_{x0}}$  = longitudinal displacement amplitude of free field (cm)  
 $u_{s_y}$  = transverse displacement of free field (cm)  
 $u_{s_{y0}}$  = transverse displacement amplitude of free field (cm)  
 $\mathbf{V}_N^R$  = state vector at the right side of pipeline  
 $\mathbf{V}^L$  = state vector at the left side of pipeline  
 $\mathbf{V}^R$  = state vector at the right side of pipeline  
 $V_s$  = shear velocity (cm/sec)  
 $v$  = transverse displacement of pipe (cm)  
 $v^L$  = transverse displacement at the left boundary of pipeline (cm)  
 $v_0(x)$  = particular solution for transverse equation of motion  
 $\alpha$  = bent angle of pipeline  
 $\beta_1$  = stiffness ratio for longitudinal motion  
 $\beta_2$  = stiffness ratio for transverse motion  
 $\epsilon_{\max}$  = maximum strain of free field  
 $\xi$  = distance results from a phase delay at the origin of  $x$ -axis (cm)  
 $\phi$  = deflection angle of pipe (rad.)  
 $\phi_d$  = diameter of pipe (mm)  
 $\theta$  = arbitrary incident angle of wave to the pipe axis (rad.)  
 $\theta_r$  = rotational joint motion (rad.)  
 $\delta_l$  = relative joint displacement (cm)  
 $\delta_l$  = relative joint displacement caused by longitudinal motion (cm)  
 $\delta_r$  = relative joint displacement caused by rotational motion (cm)  
 $\gamma_t$  = weight of soil per unit volume ( $\text{kg}/\text{cm}^3$ )  
 $\omega$  = angular frequency (rad/sec)